

# FAST NEUTRON CROSS-SECTION MEASUREMENTS WITH THE NELBE NEUTRON TIME-OF-FLIGHT FACILITY

A. Wagner<sup>1\*</sup>, D. Bemmerer<sup>1</sup>, R. Beyer<sup>1</sup>, E. Birgersson<sup>1</sup>, A. Ferrari<sup>1</sup>, E. Grosse<sup>1,3</sup>, R. Hannaske<sup>1</sup>, A. R. Junghans<sup>1</sup>, M. Kempe<sup>1,3</sup>, T. Kögler<sup>1,3</sup>, M. Marta<sup>1</sup>, A. Matic<sup>1</sup>, R. Nolte<sup>4</sup>, K. D. Schilling<sup>1</sup>, G. Schramm<sup>1,3</sup>, R. Schwengner<sup>1</sup>, F.-P. Weiss<sup>2</sup>, D. Yakorev<sup>1</sup>

<sup>1</sup>*Institute for Radiation Physics, Forschungszentrum Dresden-Rossendorf  
Postfach D-01314 Dresden, Germany*

<sup>2</sup>*Institute for Safety Research, Forschungszentrum Dresden-Rossendorf  
Postfach 510119, D-01314 Dresden, Germany*

<sup>3</sup>*Institute for Nuclear and Particle Physics, Technische Universität Dresden  
D-01062 Dresden, Germany*

<sup>4</sup>*Physikalisch-Technische Bundesanstalt  
Bundesallee 111, D-38116 Braunschweig, Germany*

## Abstract

At the Forschungszentrum Dresden-Rossendorf a new neutron time-of-flight [Klug07] facility has been set up. Fast neutrons in the energy range from 0.1 MeV to 10 MeV are produced using pulsed electron beams from a superconducting electron linear accelerator [Gabriel00]. Short beam pulses of less than 10 ps allow high-resolution time-of-flight experiments with the aim to determine interaction cross sections of neutrons with reactor structural materials and actinides at energies matching the neutron energies in fast reactors [Salvatores08].

Following experiments using a thermionic electron injector a new superconducting radio-frequency injector [Arnold07] has been built which will allow average beam currents of 0.5 mA at a repetition rate of 500 kHz.

Meanwhile, first experiments on inelastic neutron scattering cross sections on <sup>56</sup>Fe and total neutron cross sections on aluminium and tantalum have been performed as benchmark experiments. While photons from the de-exciting transitions are being detected using a 16-element BaF<sub>2</sub> scintillator array, neutrons are measured with five low-threshold plastic scintillation detectors [Beyer07]. Beam normalisation is done using a calibrated <sup>235</sup>U fission chamber. The preparation of actinide targets for neutron induced fission cross section measurements is under way.

## Experimental Setup

The radiation source ELBE (Electron Linear Accelerator with High Brilliance and Low Emittance) at Forschungszentrum Dresden-Rossendorf (FZD) makes use of a superconducting continuous-wave electron linear accelerator delivering beams with energies up to 50 MeV. The high-intensity beam with average beam currents of up to 1 mA at pulse repetition rates up to 26 MHz serves as a driver for the production of various secondary beams. Figure 1 shows the layout of the accelerator facility and the beam lines for secondary radiations. Table 1 lists the available secondary beams and their primary applications. As one of the secondary beams, an intense neutron beam is being produced by bremsstrahlung photons via the ( $\gamma, n$ )-process inside a liquid-lead circuit. The lead acts threefold as the electron-to-bremsstrahlung convertor, as the source of evaporation neutrons, as well as the heat removal medium in order to cope with the designed average electron beam power of

---

\* Corresponding author: a.wagner@fzd.de

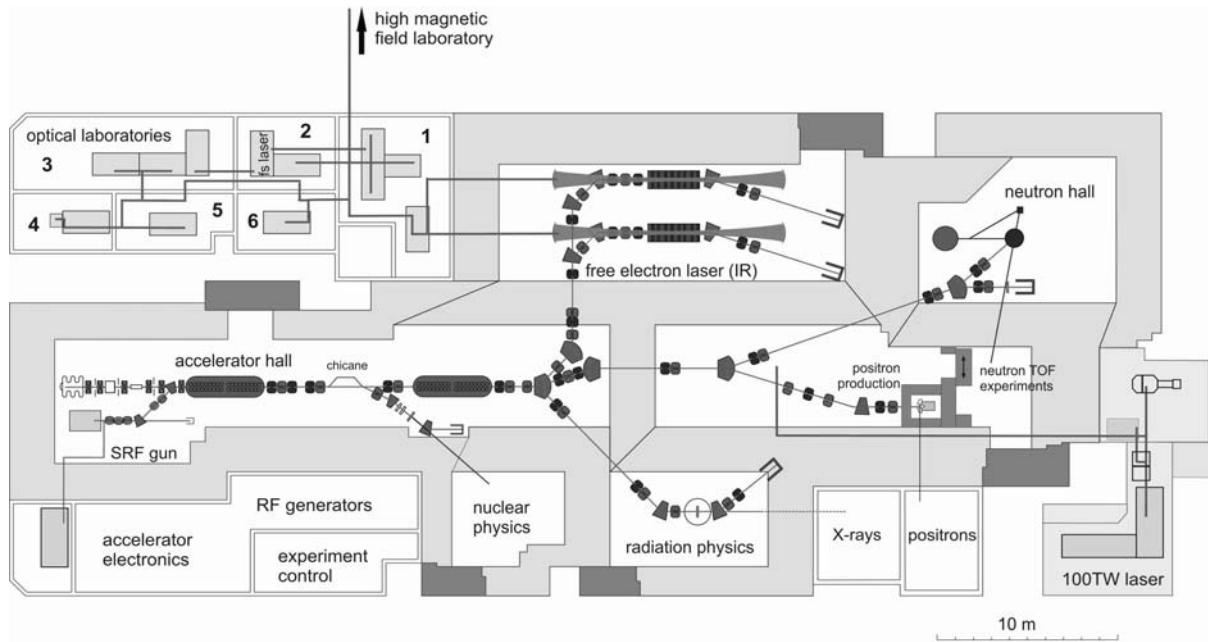


Fig. 1: *Layout of the accelerator facility ELBE. Two superconducting accelerator structures are located inside the accelerator hall and the liquid-lead loop is situated on the upper right side inside the neutron hall. A new superconducting radio-frequency injector is already installed (SRF gun) which will allow for increase in electron bunch charge by a factor of 15 as compared to the standard thermoionic injector. Recently, a 100 TW laser systems has been set up which serves for laser-Thomson electron-scattering experiments and laser-plasma particle acceleration experiments.*

about 50 kW. Monte Carlo simulations using MCNP and GEANT4 were performed to characterise the neutron and photon intensities as well as time and energy distributions, and to optimise the neutron transport and shielding of the experimental setup.

The design of the liquid-lead loop is shown in Fig. 2. The design focuses on combining a small active volume of neutron production with a correspondingly high local heat load of about 5 kW / g. As one of the possible solutions, a liquid-lead loop operated at a temperature of about 630 K has been selected which is also favourable by means of induced radioactivity caused by various  $(\gamma, xn)$ - and  $(\gamma, p)$ -reactions as compared to e.g. liquid mercury.

Nevertheless, the liquid-lead loop has to be stored during shutdown phases inside a lead shielding of 200 mm thickness in order to grant access to the vault for maintenance and other experiments [Seidel07]. While using lead as material for efficient neutron production (neutron separation energies  $S_n$  from 6.7 to 8.1 MeV) the beam dump is made from pure aluminium (>99.9%) resulting in low induced activities and low neutron generation (neutron separation energy of  $^{27}\text{Al}$ :  $S_n=13.1$  MeV).

The short beam pulses (about 5 ps FWHM) delivered by the superconducting electron accelerator provide the basis for an excellent time resolution for neutron time-of-flight experiments while the pulse repetition rates can be varied between 100 kHz and 26 MHz according to the demands of the experiments. With the existing electronically pulsed thermionic electron source electron pulse charges of up to 80 pC are realized allowing for a moderate average electron beam current of 16  $\mu\text{A}$  at a repetition rate of 200 kHz.

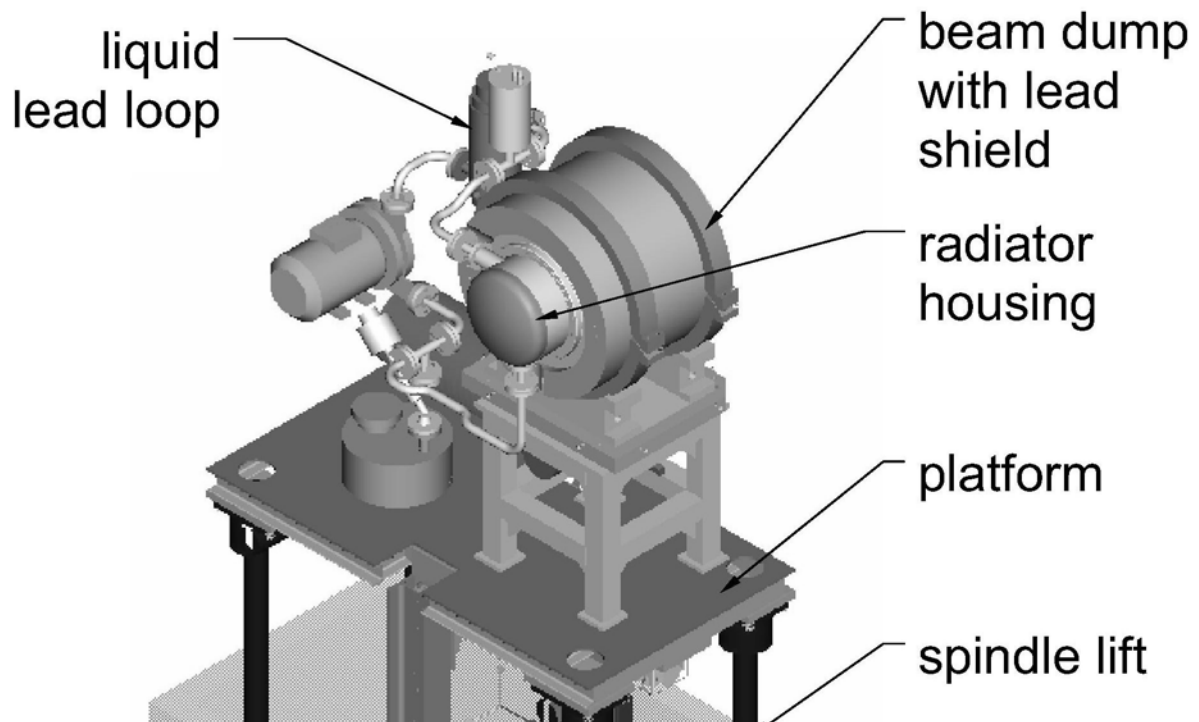


Fig. 2: Three-dimensional rendering of the liquid-lead loop installed at the ELBE facility. For reasons of radiation protection the platform containing the lead loop can be lowered into a lead housing by means of a remotely controlled spindle lifter. The intense electron beam impinges from the front left while the beam transport system is not shown here. The lead flow is driven by means of a magneto-hydrodynamic pump thus avoiding mechanical contact with the fluid and avoiding mechanical feedthroughs. Thermal insulation, heating units, and support systems are not shown. The beam dump is made from aluminium surrounded by lead in backward and radial directions.

A new superconducting radio-frequency injector is already installed which in the near future will allow for an increase in electron bunch charge by a factor of 15 and repetition rates of 500 kHz. The short beam pulses together with the small neutron-production volume in the lead circuit allow for an energy resolution of about 1% with a flight path of 6 m when using a fast detector stop signal (e.g., 1 ns for 1.5 MeV neutrons).

Neutrons emerging from the liquid-lead radiator are shaped into a beam using a 240 cm long cylindrically symmetric collimator made from borated polyethylene and lead, greatly reducing scattered-neutron background and photons at the target position.

Around the target, an array of 16 BaF<sub>2</sub> scintillation detectors for the detection of secondary photons has been installed. Each detector consists of two 190 mm long prisms with hexagonal bases of 53 mm inner radius glued together and read out on both ends using fast photomultiplier tubes<sup>†</sup> (PMT). The double-sided readout helps to reduce background signals stemming from anode dark-currents, it improves the energy resolution, and it permits the determination of the longitudinal hit position. The signals from the PMTs are processed in

<sup>†</sup> Hamamatsu Photonics K.K., <http://www.hamamatsu.com>, PMT: R2059-01 selected with quartz windows.

dedicated VME-based readout units allowing for pulse-shape discrimination of charged particles and photons.

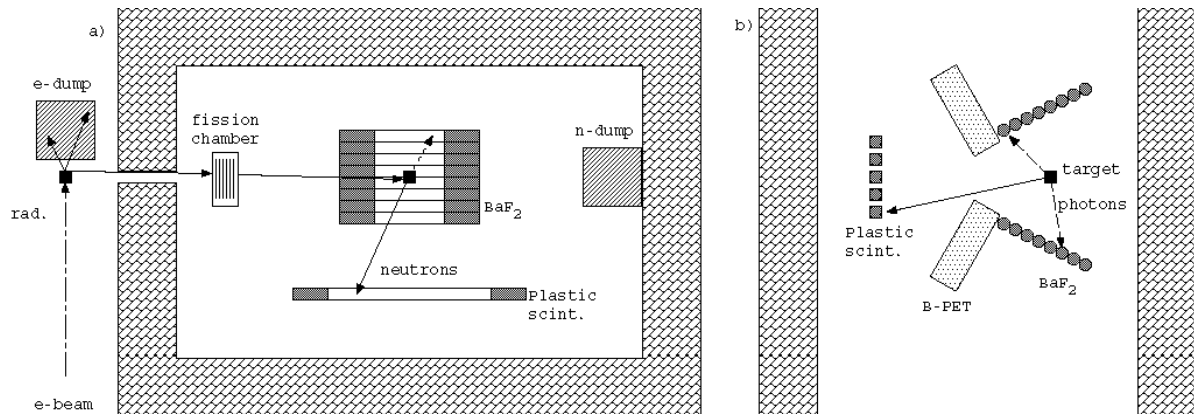


Fig. 3: Sketch of the setup used in neutron inelastic scattering experiments. Part a) shows the top view, and part b) shows the side view of the detector and target arrangements. Solid (dashed) lines refer to neutron (photon) tracks. Electron-optical elements are not shown. Drawing is not to scale.

Scattered neutrons are detected using proton-recoil plastic scintillation detectors at a distance of about 1 m from the target. The plastic scintillation detectors are strips<sup>‡</sup> of 1000 mm length and 42 mm x 11 mm cross section read-out double-sided using the same PMTs as described above. The trigger threshold is selected to detect single photo-electrons permitting detection limits for neutrons as low as 30 keV for detection efficiencies above 10%. The design, operation, and calibration of these detectors are described in a previous publication [Beyer07]. The system is optimized for high time resolution of the time-of-flight detectors reaching about 600 ps FWHM for the BaF<sub>2</sub>-detectors and about 860 ps FWHM for the plastic scintillation detectors in order to allow a compact setup ensuring high beam repetition rates with low pulse-to-pulse overlap. Scattered neutrons and photons originating from the BaF<sub>2</sub>-array are being suppressed by borated polyethylene absorbers in the direction of the neutron detectors. The distribution of random background has been determined in measurements without target. Neutron flux determination is done using a calibrated U-235 fission chamber [Gayther90]. The time resolution obtained using photo-induced fission amounts to about 4 ns. The data-acquisition system is controlled by a VME-based computer<sup>§</sup> running the real-time operating system LynxOS and the versatile data acquisition system MBS<sup>\*\*</sup>. The readout of the double-sided BaF<sub>2</sub>-detectors is done using CAEN<sup>††</sup> V874b calorimeter units providing the energy information, while the plastic-scintillation neutron-detector information is processed by in-house made constant-fraction discriminators. CAEN V1190a time-to-digital converters provide the timing information for both detectors.

<sup>‡</sup> Eljen Technology, <http://www.eljentechnology.com>, EJ-200 scintillator.

<sup>§</sup> Creative Electronics Systems, <http://www.ces.ch>, RIO3 8064 single board computer.

<sup>\*\*</sup> GSI Multi-Branch System, <http://daq.gsi.de>.

<sup>††</sup> CAEN s.p.A., <http://www.caen.it>

## Experiments

Several experiments on interactions of fast neutrons with materials of interest for fast reactors have been performed. As a preliminary example, the inelastic scattering on iron with natural isotopic composition has been studied. Although iron is not a material of interest for transmutation studies, its importance as structural material demands high-precision data for the interaction of fast neutrons occurring in fast reactors, transmutation facilities, or accelerator-driven systems [Salvatores08]. The detector setup is shown in Figure 3. List-mode data are taken for coincident signals in the BaF<sub>2</sub>-array and the neutron-detector array selecting primarily reactions with at least one photon and one neutron in the exit channel. Time-of-flight calibration is done using the photon flash stemming from scattered bremsstrahlung inside the radiator. The target consisted of a cylindrical slab of natural iron (isotopic composition: 5.85% <sup>54</sup>Fe, 91.75% <sup>56</sup>Fe, 2.12% <sup>57</sup>Fe, 0.28% <sup>58</sup>Fe) with a mass of 19.82 g. The average neutron intensity on target amounts to about 40000 s<sup>-1</sup>cm<sup>-2</sup>.

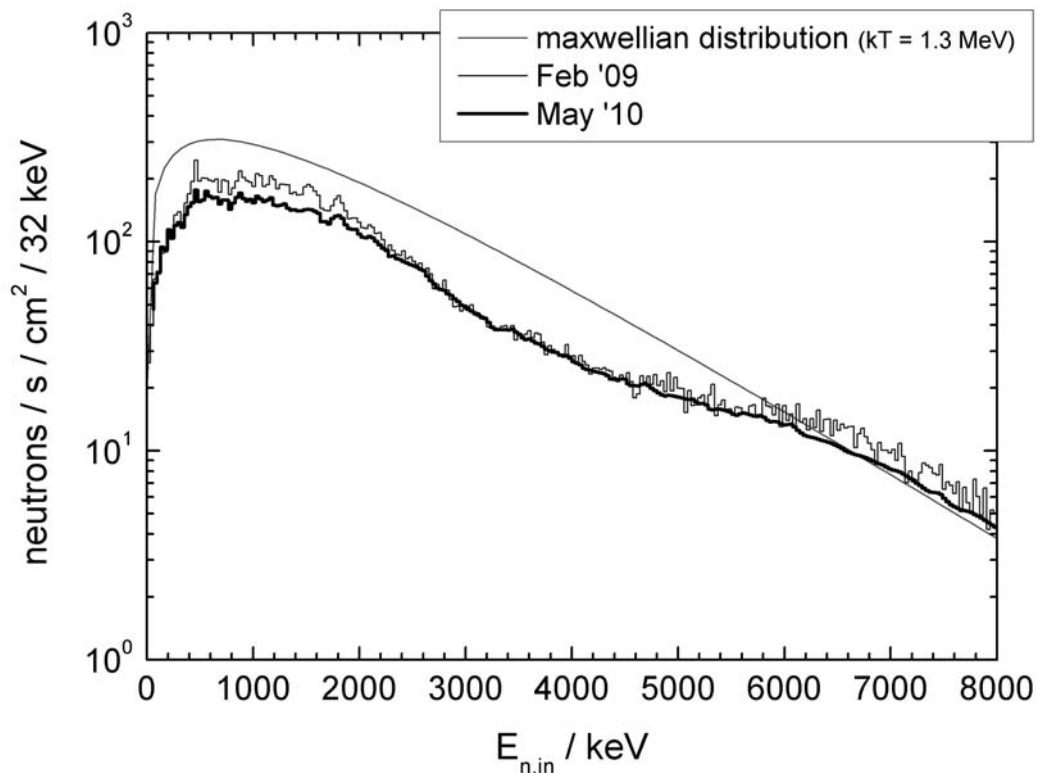


Fig. 4: Neutron flux as a function of kinetic energy determined using a <sup>235</sup>U fission chamber. Improvements in background reduction causing two different flux distributions are shown for two runs in February 2009 and May 2010. Experimental background was subtracted. Thermal neutrons account for less than 10<sup>-6</sup> of all neutrons.

## Results

Figure 4 shows the neutron energy distribution measured using the <sup>235</sup>U fission detector in time-of-flight mode. Thermal neutrons occur on a level below 10<sup>-6</sup>. Figure 5 shows the correlation of neutron velocities measured ( $\beta_{in}$ ) before and after ( $\beta_{out}$ ) scattering at the target. Velocities are measured using the timing signals of the BaF<sub>2</sub>-detectors, plastic neutron detectors, and the reference signal of the accelerator radio-frequency. Path length variations have been accounted for. While the neutrons undergo inelastic scattering events in the target, their velocity is reduced accordingly. Because the measurement is kinematically complete, the

excitation of the first excited states of the various isotopic components can be studied in detail without being limited to the first excited state as in experiments where only the decay photon or the scattered neutron is detected. Furthermore, targets of natural isotopic composition can be used eliminating the use of isotopically enriched targets. In comparison with monoenergetic neutron sources the white spectrum employed here offers the advantage of simultaneous measurements of the energy range of importance for fast reactors.

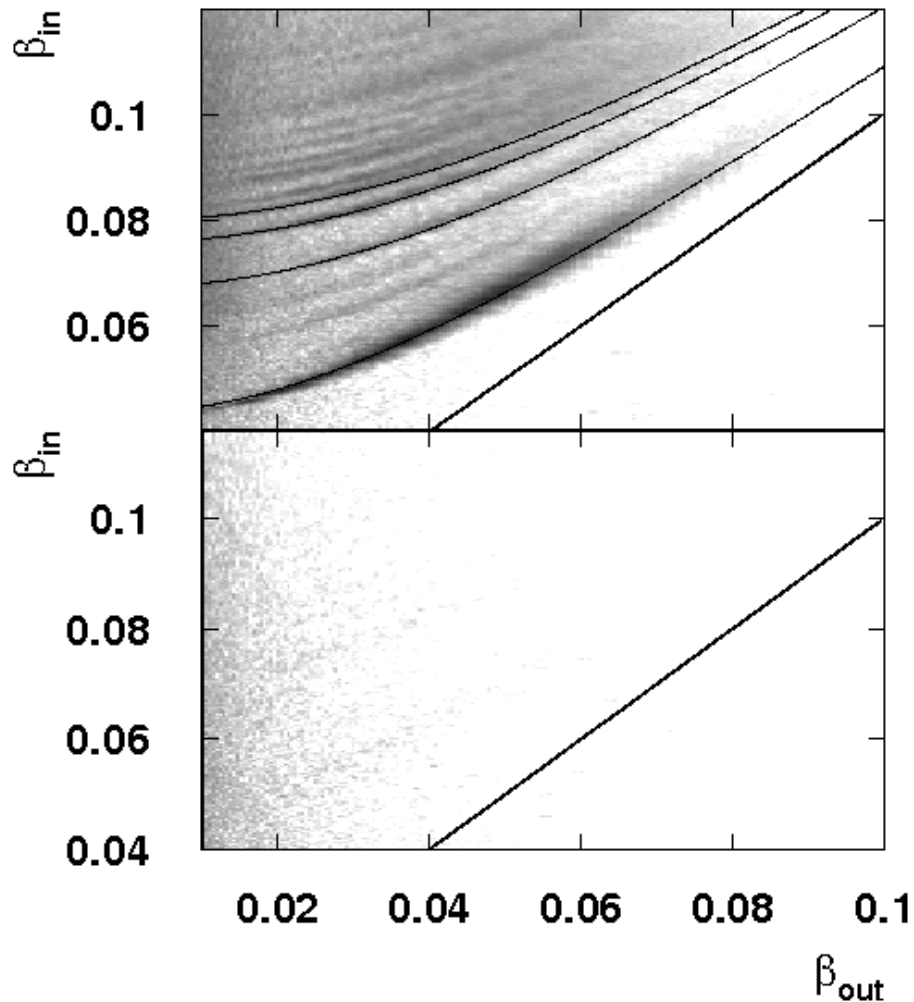


Fig. 5 Velocity correlations for neutron inelastic scattering from iron of natural isotopic abundance. The upper (lower) part shows the result for inserted (empty) target. The straight line shows the correlation for elastic scattering while the curves in the upper part indicate the first four excited states in  $^{56}\text{Fe}$ . Structures appearing between those curves belong to the first excited states in  $^{54}\text{Fe}$  and double excitation of  $^{56}\text{Fe}$ , respectively.

By gating on the neutron energy loss corresponding to a given excited state, the cross section for this particular channel can be extracted. Figure 6 shows the preliminary result for the first excited state in  $^{56}\text{Fe}$  at 847 keV. The data have been analysed assuming isotropic angular distributions of outgoing neutrons and photons. Since the photon detector covers a polar angular range of about  $\pi/4$  to  $3\pi/4$  with respect to the beam, the total cross section data will have to be corrected for neutron and photon angular distributions.

The data are in fair agreement with earlier measurements up to the energy of the second excited state in  $^{56}\text{Fe}$  [Perey71].

## Outlook

Work is still in progress to determine precise cross section taking into account detector efficiencies, angular distributions of neutrons and photons, incident neutron flux densities, and contributions from room background. Starting in September 2010, the new superconducting radio-frequency injector will be commissioned for routine operation.

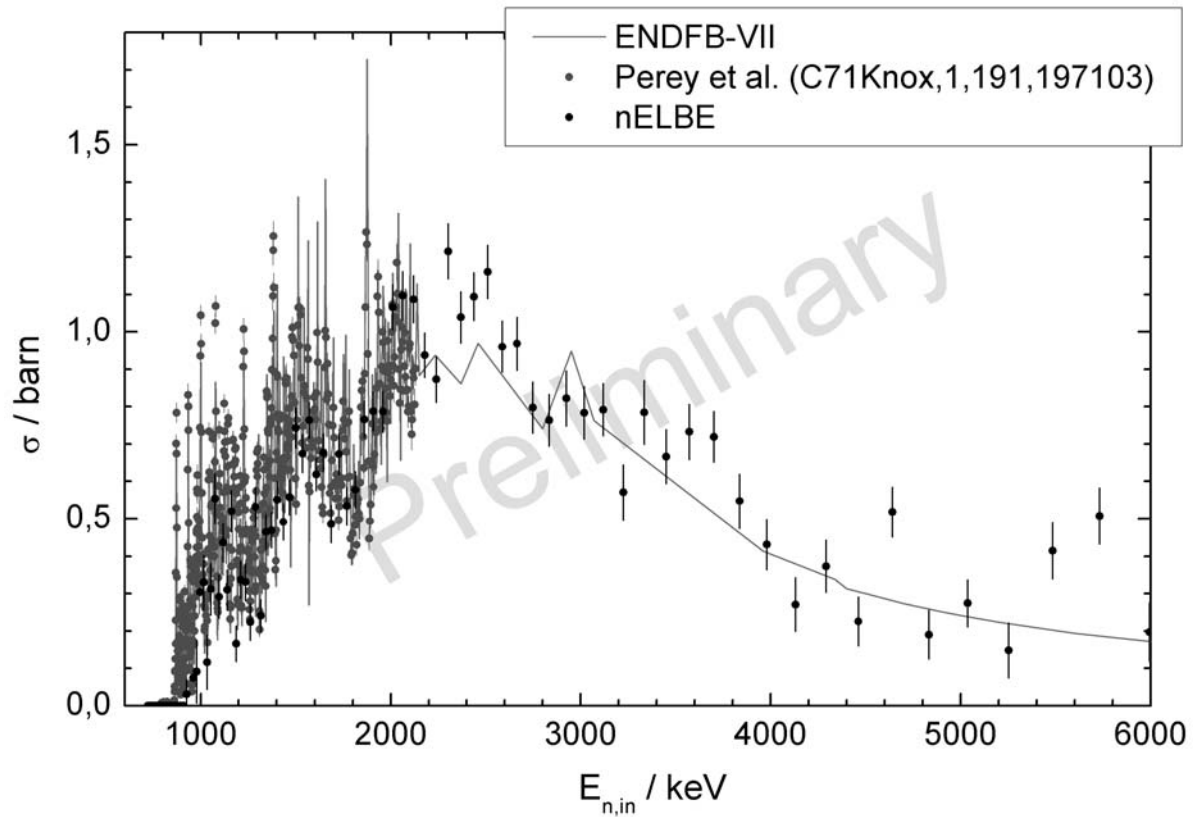


Fig. 6: Preliminary results for the cross section for the direct excitation of the 847 keV level in  $^{56}\text{Fe}$  in kinematically-complete inelastic neutron scattering (solid black points). The line shows the estimate from the ENDF library. Grey points below an energy of 2.1 MeV show data taken in scattering experiments where only the outgoing photon is detected [Pery71].

## Acknowledgments

The project is supported by European Commission under the FP6- I3 program EFNUDAT (FP6-036434), the Deutsche Forschungsgemeinschaft (FR 575/5, GR 1674/2), and the German Federal Ministry of Education and Research (02NUK13). The authors would like to thank the ELBE-crew for providing the electron beams and M. Sobiella and A. Hartmann for continuous technical support.

## References

- [Klug07] J. Klug, E. Altstadt, C. Beckert, et al., Nucl. Instr. Meth. A 577 (2007) 641  
 [Altstadt07] E. Altstadt, C. Beckert, H. Freiesleben, et al., Annals of Nuclear Energy 34 (2007) 36–50  
 [Gabriel00] F. Gabriel, P. Gippner, E. Grosse, et al., Nucl. Instr. Meth. B 161 (2000) 1143  
 [Arnold07] A. Arnold, H. Büttig, D. Janssen, et al., Nucl. Instr. Meth. A 577 (2007) 440  
 [Beyer07] R. Beyer, E. Grosse, K. Heidel, et al., Nucl. Instr. Meth. A 575 (2007) 449  
 [Seidel07] K. Seidel, P. Batistoni, U. Fischer, et al., Fusion Engineering and Design 82 (2007) 2212  
 [Gayther90] D.B. Gayther, Metrologia 27 (1990) 221  
 [Salvatores08] M. Salvatores, NEA-Report No. 6410, 2008 and <http://www.nea.fr/science/wpec/volume26/volume26.pdf>  
 [Perey71] F.G. Perey, W.E Kinney, R.L. Macklin, Proc. 3<sup>rd</sup> Int. Conf. Neutron Cross Sections + Tech. (1971) 191

Table 1: Available beams at the superconducting electron accelerator ELBE, the type of radiation, and the primary application.

Secondary beam	Radiation	Application
Free-Electron Laser	Coherent infrared light, wavelength range from 3-230 $\mu\text{m}$	IR spectroscopy in semiconductors, quantum systems, soft matter, biological systems
Channelling radiation	Quasi-monochromatic X-rays, 10 – 100 keV	Cell survival and damage studies of low-energy X-rays
(Polarized) Bremsstrahlung	Broad-band high-energy photons, 0 – 20 MeV	Nuclear astrophysics and transmutation-related ( $\gamma, \gamma$ )- ( $\gamma, n$ )-, ( $\gamma, p$ )-, ( $\gamma, \alpha$ )-reactions, materials research with positrons
Positrons	Mono-energetic positrons, 0 – 50 keV	materials research with positrons, defect studies in thin films and bulk materials
Neutrons	Evaporation neutrons produced in ( $\gamma, n$ )-processes, 200 keV – 10 MeV	Total and inelastic neutron reaction cross sections for reactor materials and nuclear transmutation
Electrons	Direct beams of 6 MeV – 40 MeV	Detector tests with < 10 ps timing resolution and intensities from one up to $10^5 \text{ s}^{-1} \text{ cm}^{-2}$